

**2<sup>nd</sup>** PANHELLENIC CONGRESS OF MEDICAL PHYSICS  
4-6 OCTOBER 2024 | EUGENIDES FOUNDATION

# Nanoparticle-based gas sensors with potential for biomedical applications

E. Karadimas<sup>1</sup>, E. Skotadis<sup>1 2</sup>, D. Tsoukalas<sup>2</sup>, M. Kallergi<sup>1</sup>

<sup>1</sup> Department of Biomedical Engineering, University of West Attica, 12243 Egaleo, Greece

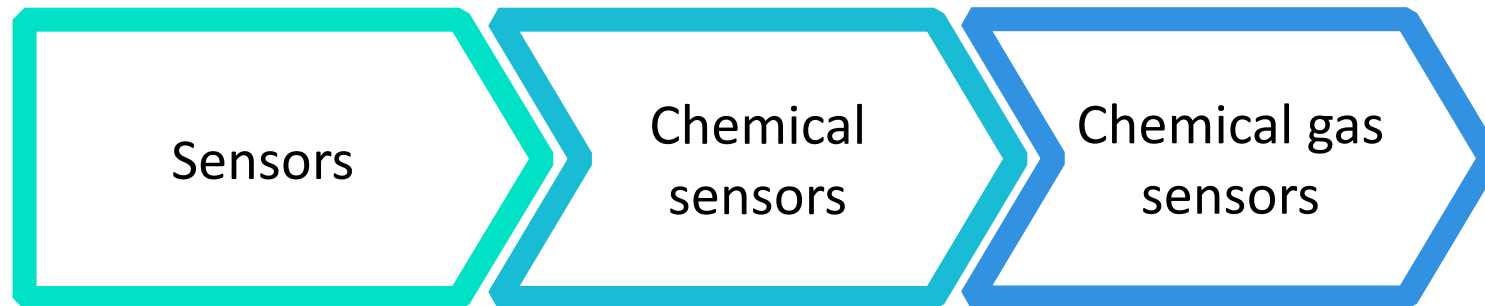
<sup>2</sup> School of Applied Mathematical and Physical Sciences, National Technical University of Athens, 15780, Zografos Campus, Greece

# 1. Background-Aim

## Chemical gas sensors

Chemical gas sensors aim to detect specific molecules of a target gas and are often referred to as electronic noses. These sensors are of great interest for biomedical applications and the detection of gaseous biomarkers such as specific gas molecules found in human breath.

### Classification of Sensors Based on the Transducer



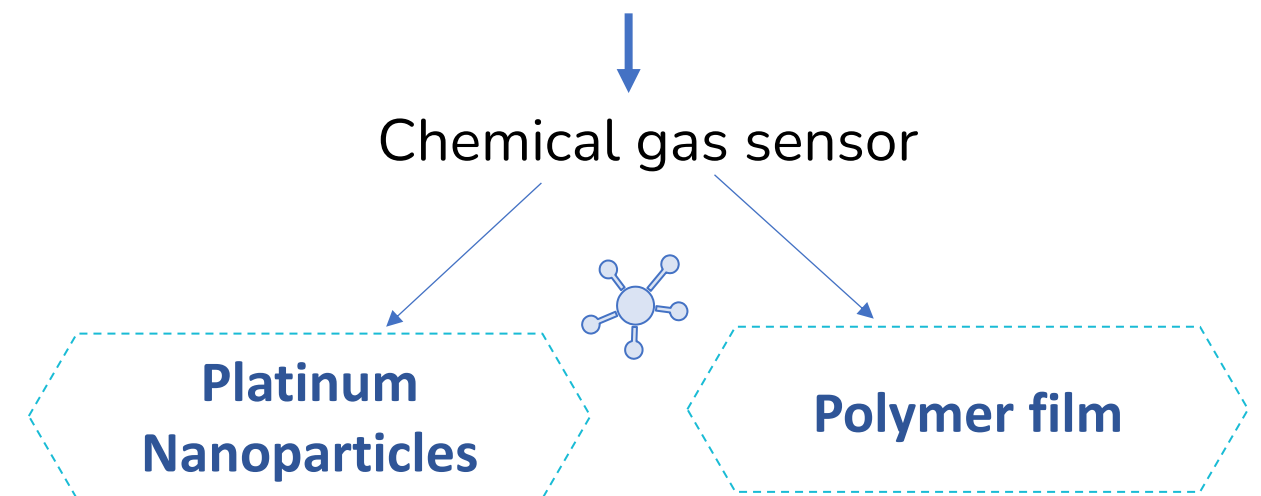
### Classification of Sensors Based on the Sample



## Nanoparticle-based gas sensors

The adsorption and diffusion of gases by polymers, as well as the conductivity mechanisms governing nanoparticles, make the sensor suitable for this specific application.

### Detection of Volatile Organic Compounds in Common Pesticides



Sensor-conductivity can be modified dependent on gas concentration, temperature and humidity.

## 2. Materials & Methods

### Nanoparticle based Sensor

Platinum nanoparticles having a mean diameter of 4 nm have been deposited on top of oxidized silicon substrates, previously patterned with gold IDEs (Fig.1) using a modified magnetron sputtering system (Fig.2). Solutions of four polymers, Poly(ethyl methacrylate) (PEMA), Poly(2-hydroxyethyl methacrylate) (PHEMA), poly(isobutyl methacrylate) (PIBMA) and poly(butyl methacrylate) (PBMA). All polymeric solutions were prepared using a high precision micro-balance and PGMEA as a solvent. The solutions treated in an ultrasonic bath for 2 h. The resulting polymer-PGMEA solutions were then spin-coated on top of the nanoparticle Here all of the abovementioned results are taken into account: all of the sensors used in the current experimental setups were designed with an IDE inter finger spacing of 10  $\mu\text{m}$  and a nanoparticle surface coverage of 46%.

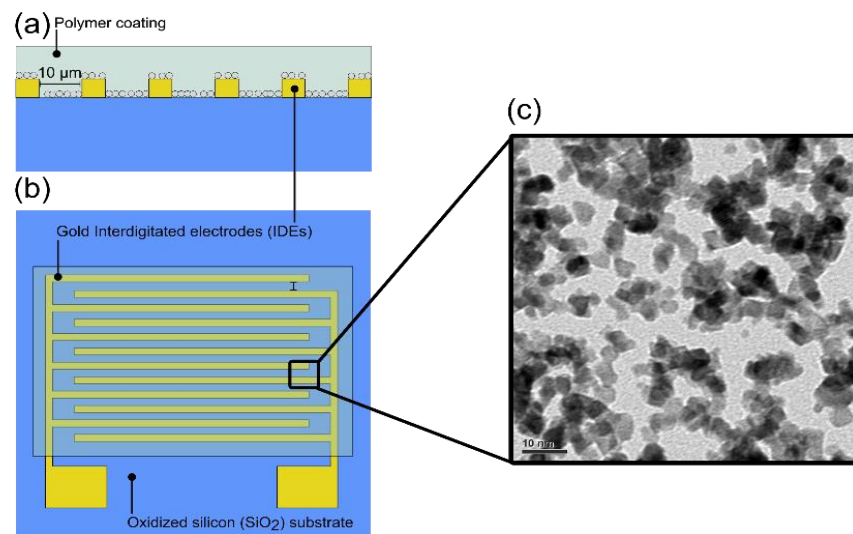


**Fig. 2.** (Skotadis, E. et al., 2020)

(a) cross section of the sensing device (b) Top-down view of the sensor (c) Transmission Electron Microscopy Image

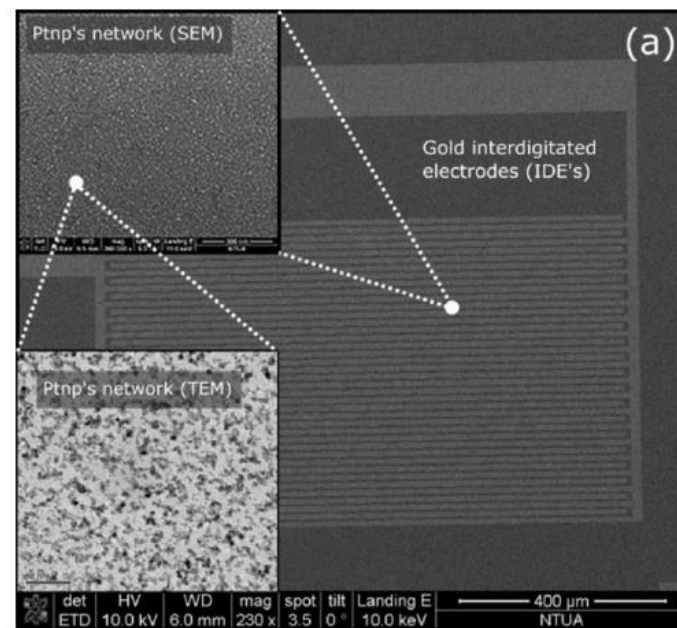
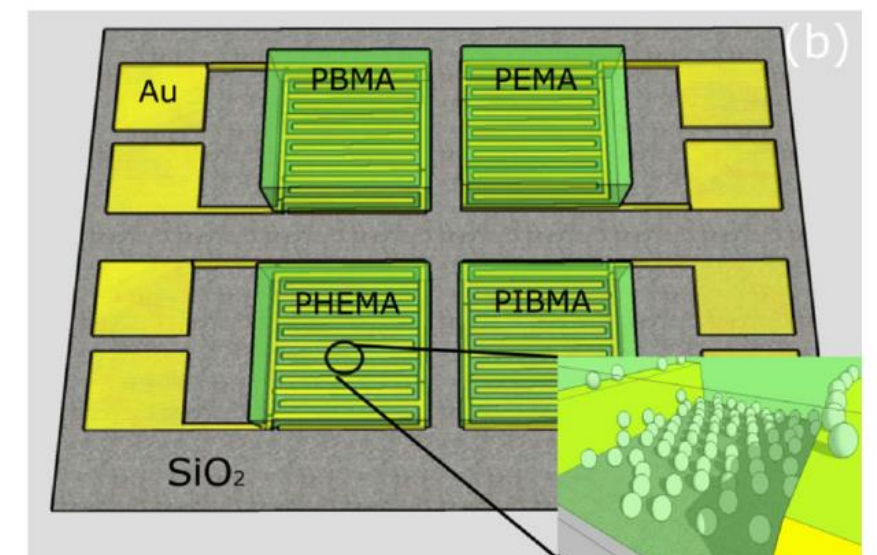


**Fig. 1.** (Madianos, et al., 2018)

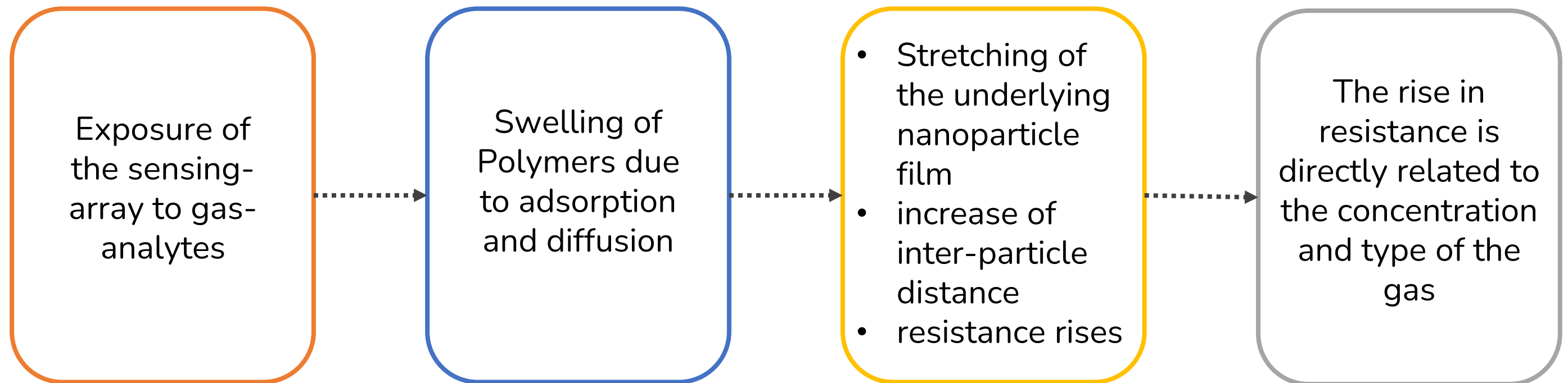
(a) SEM image of the nanoparticles



(b) Schematic of the finalized pesticide gas-sensors

## 2. Materials & Methods

### Operating Principle



### Experimental analysis

The sensing array can identify and quantify two gas-analytes, one pesticide solution, and relative humidity, which acts as a reference analyte. All the evaluation experiments were conducted in close to real-life conditions; specifically, the sensors response towards the analytes was tested in three relative humidity backgrounds 60, 70 and 90% while the effect of temperature was also considered (25°C and 35°C).

## 2. Materials & Methods

The sensors were exposed to different concentrations of the pesticide/analyte in relation to humidity. Specifically, 50 mL of Nimrod test solution was placed in one bubbler, while another bubbler contained 50 mL of deionized (DI) water as a reference analyte (Fig. 3). Vapours from both bubblers were collected by supplying them with separate nitrogen gas lines, each controlled externally by three Nitrogen Mass Flow Controllers (MFCs). The final gas mixture introduced into the sensing array's measurement chamber had a composition based on the partial vapor pressures of the solution's components. Different concentrations of Nimrod or humidity, achieved by adjusting the nitrogen flow rates, were overlaid onto a constant background flow of nitrogen and 50% humidity, which was then delivered to the sensors' measurement chamber.

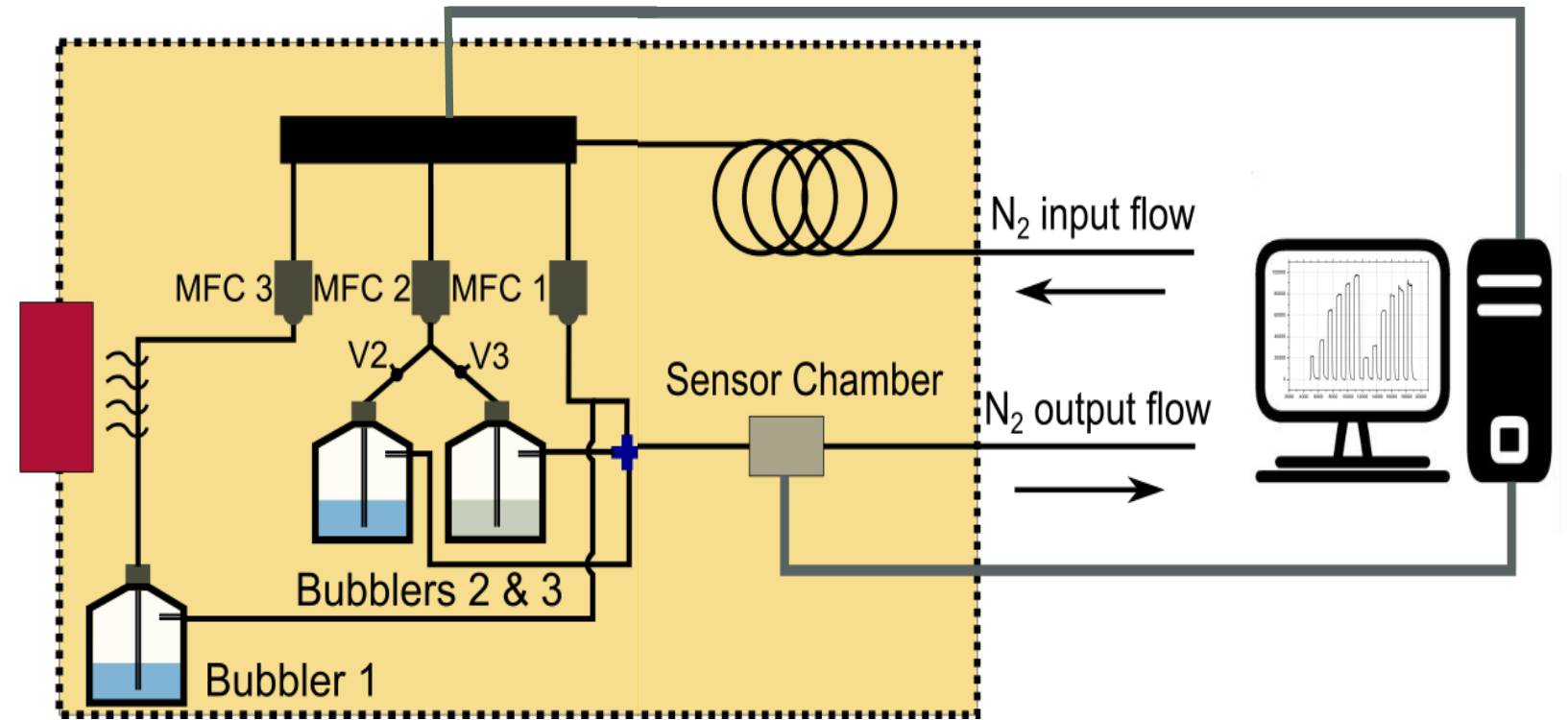


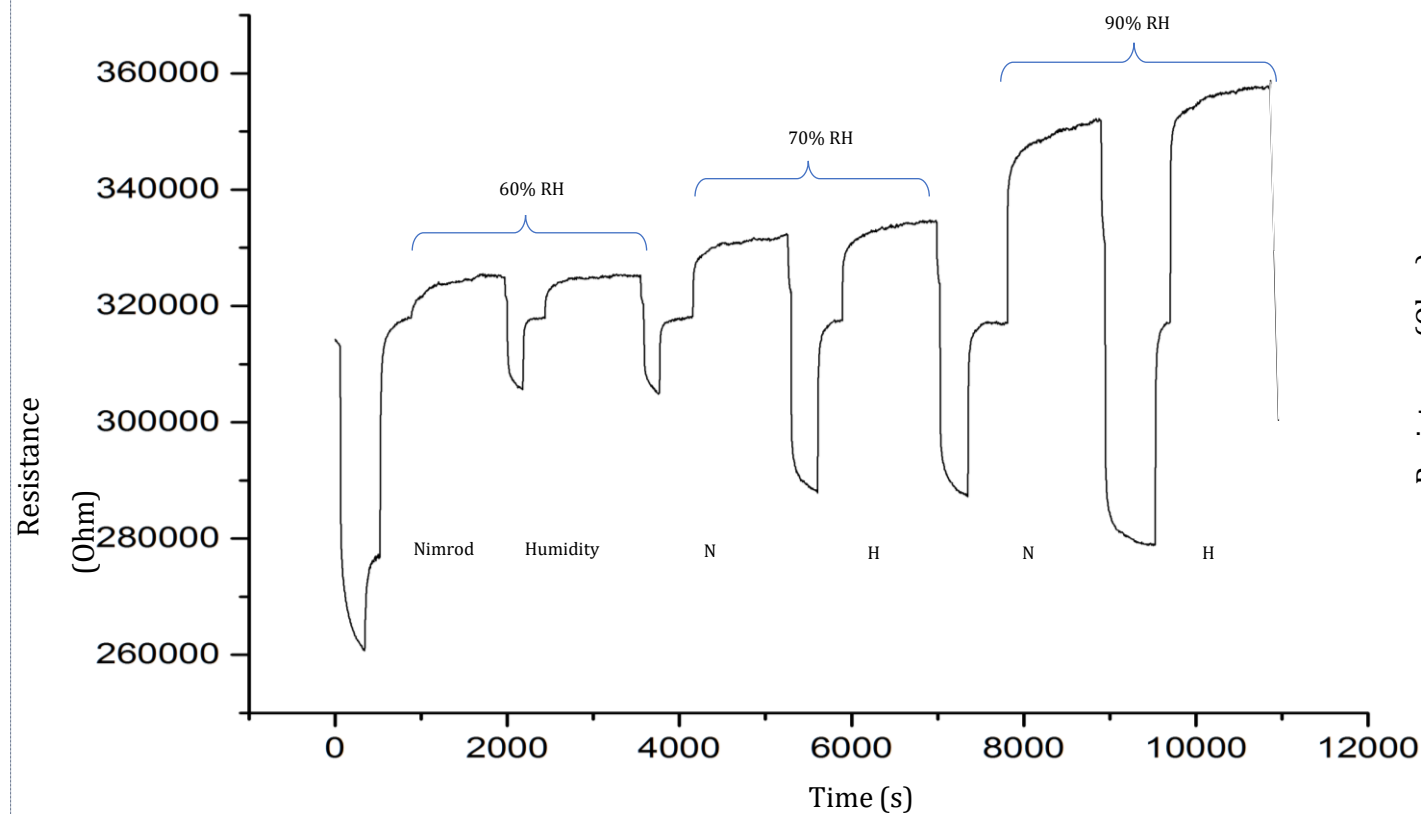
**Fig. 3.** (Skotadis, E. et al., 2020)

The Schematic of the experimental, gas sensor characterization setup can be shown in Fig.3. MFCs are controlled via A PC and a labview program. A heating element is used to increase the temperature. In addition, a high-resistance multimeter (Keithley 2400) was used.

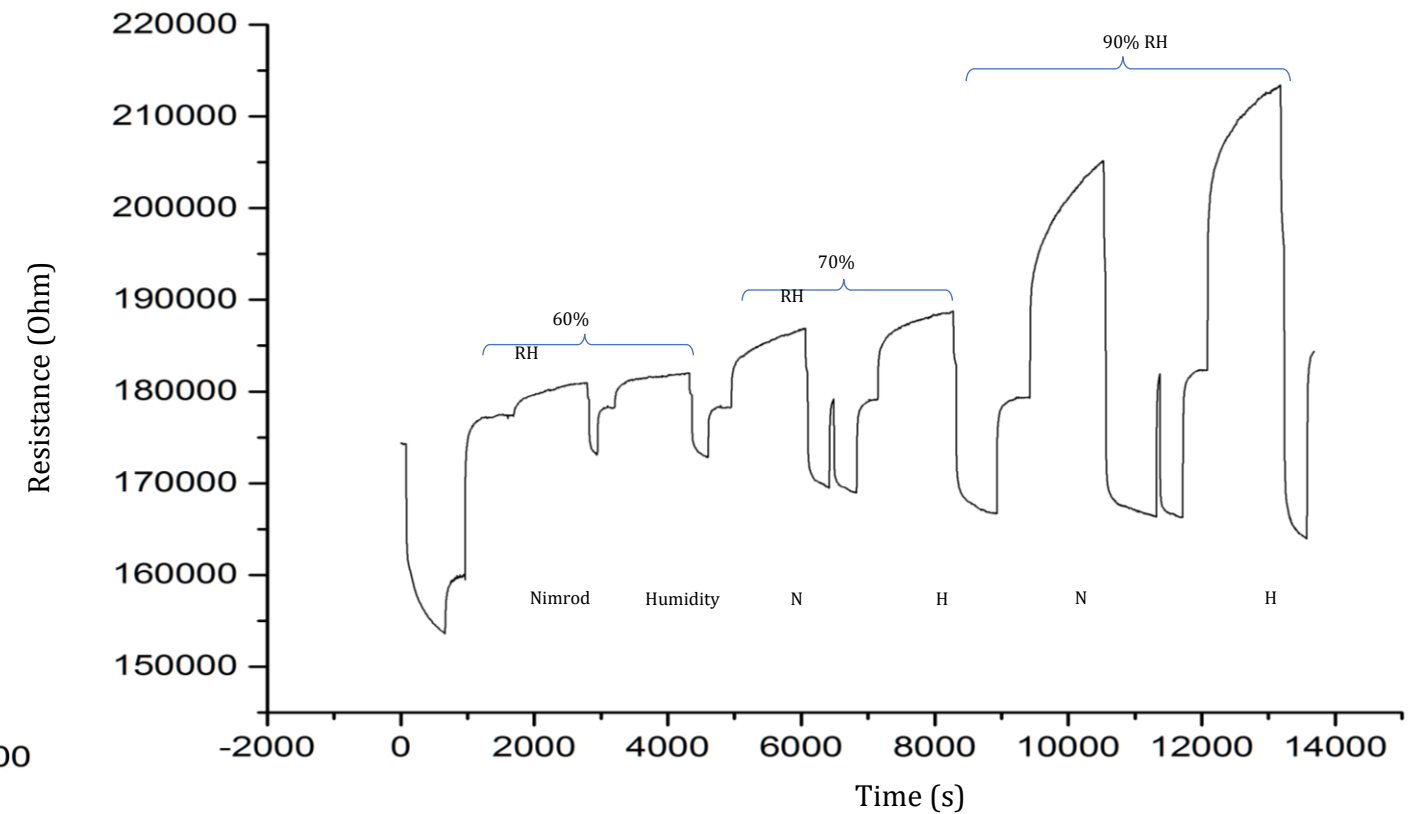
### 3. Results

## Dynamic Response

The dynamic response of the sensors, across all measurements, can provide a general overview and direction for the results of the experimental measurements. Specifically, the response of the sensors can be observed on a large scale as the peaks and resistance values are compared for the different experimental conditions. Since the initial resistance values of the sensors were re-evaluated before each measurement, it would be safe to assume the following: the change in resistance, under the same experimental conditions, is different in the case of pesticide flow and different in the case of humidity flow. Thus, this is a way to distinguish between them. Graph 1 and 2 presenting the PEMA sensors' response at two different temperatures.



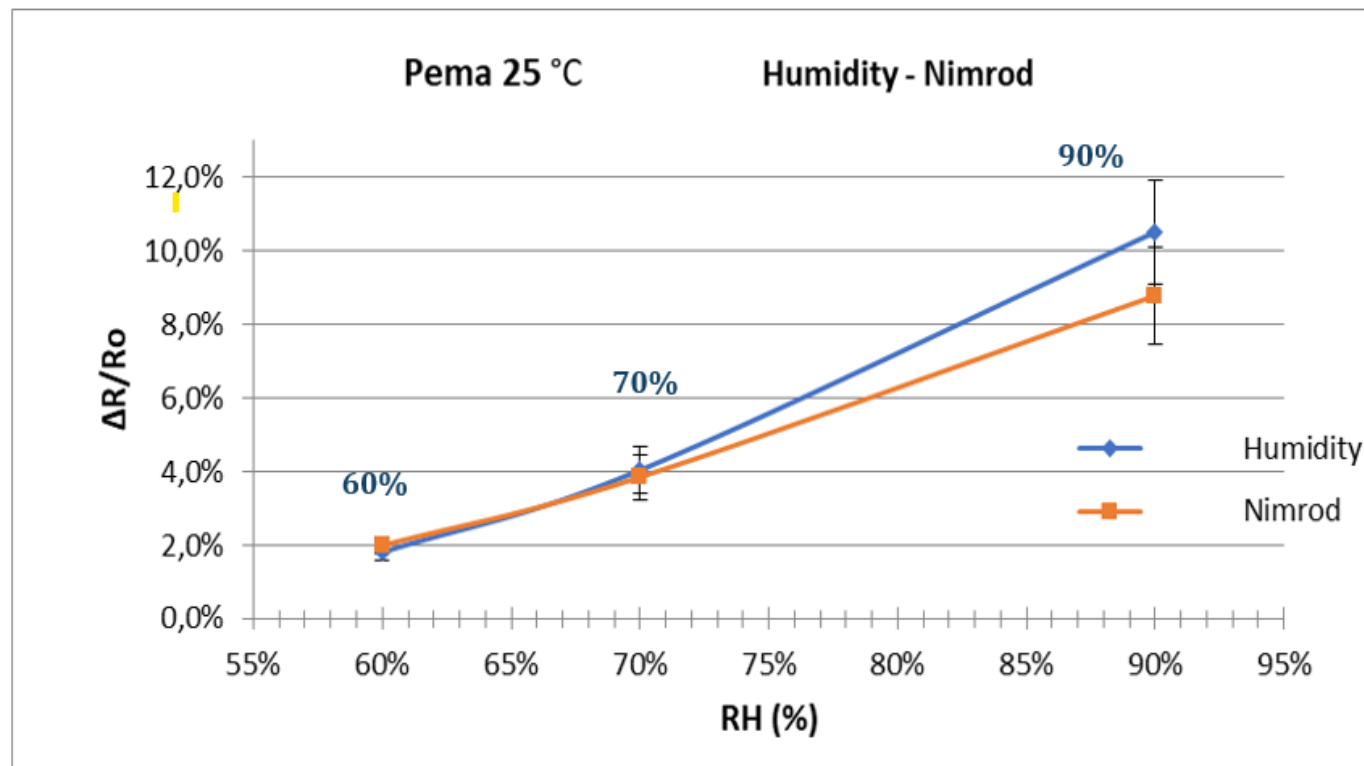
**Graph.1.** Dynamic response of the Pema sensor at 25 °C



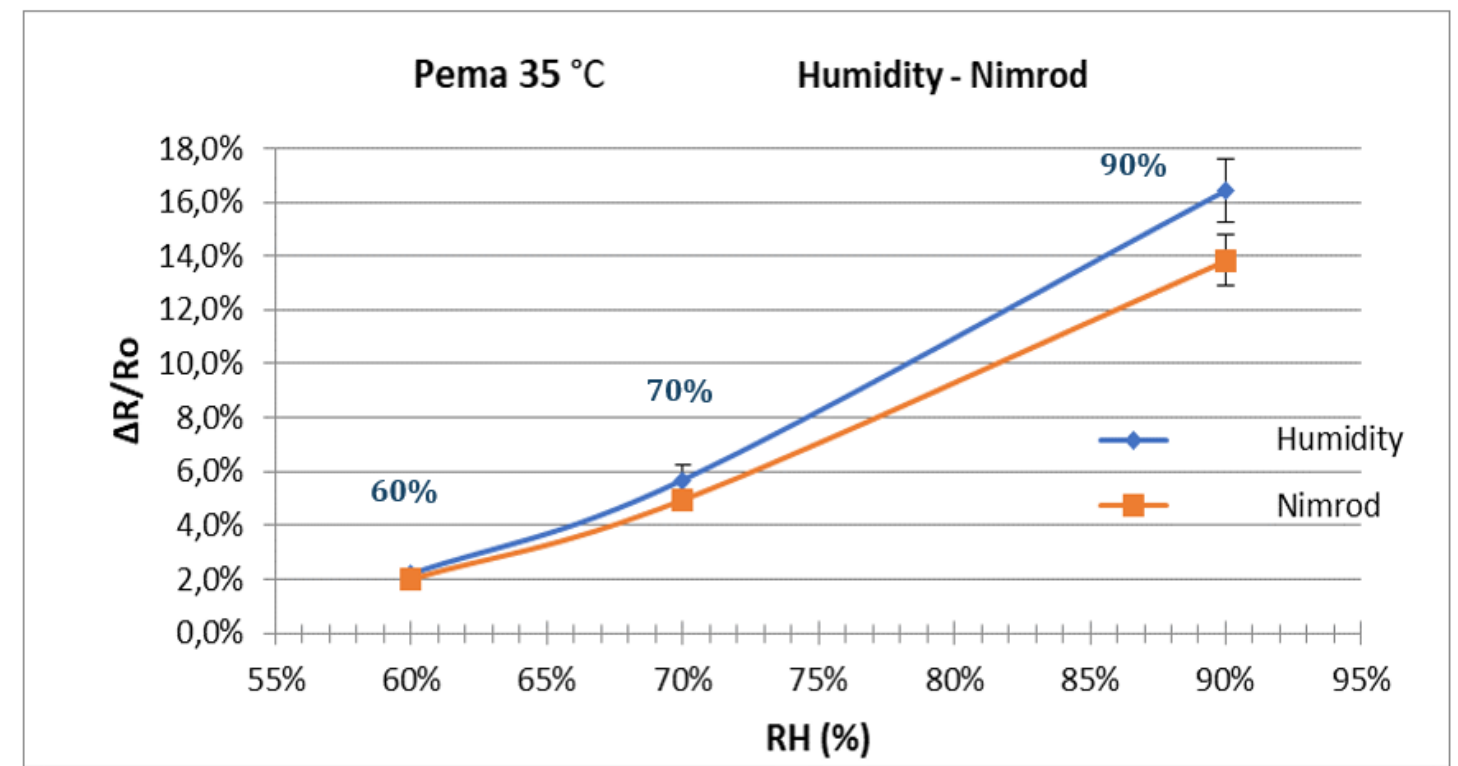
**Graph.2.** Dynamic response of the Pema sensor at 35 °C

### 3. Results

The optimal way to record measurements is to log the initial and final resistance values for pesticide flow and humidity. The percentage change in resistance was calculated  $(\Delta R/R_0)\%$ . The following graphs show  $(\Delta R/R_0)\%$  as a function of Gas concentration. It is important to note the following: Since we are unable to determine the exact concentration of Nimrod while increasing the nitrogen flow, we instead report the humidity concentration at the same flow rate (Graphs 3 and 4).



**Graph.3.** Average response of the Pema sensor at 25 °C.



**Graph.4** Average response of the Pema sensor at 35 °C.

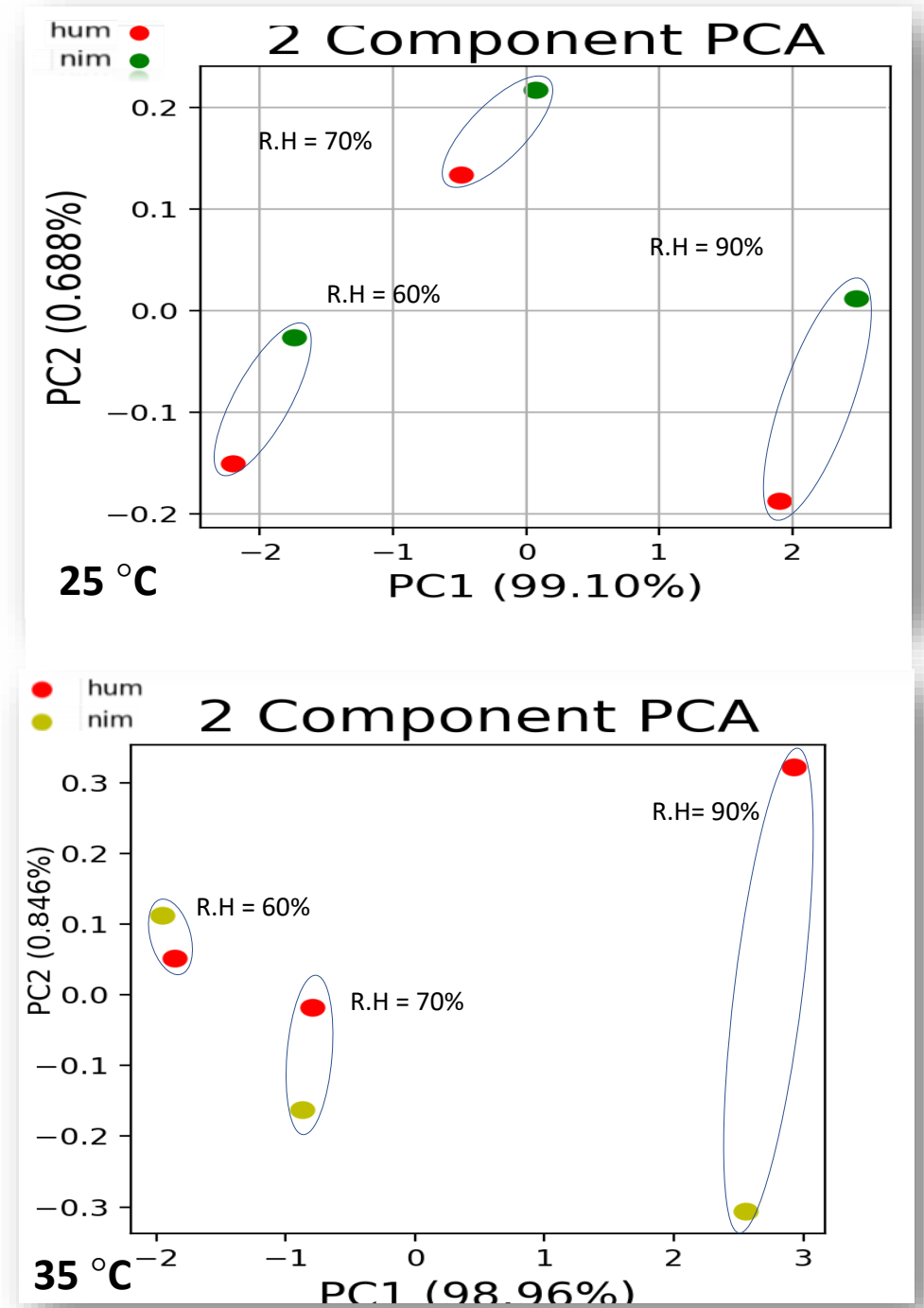
## 4. Conclusions

### PCA Analysis

As a final step, the data-set has been processed using the Principal Component Analysis (PCA) method. The maximum variances of the data are used as the basis for the creation of the new system.

The PCA outcomes are shown following the array's response to Nimrod against relative humidity (R.H.), with a constant R.H. background of 50% maintained throughout, and at two temperatures (25°C and 35°C). The array exhibits varied reactions depending on whether the pesticide is present or not. This is evident in the PCA data points, which remain distinct and never overlap. (Refer to Figures 5 and 6). Such differentiation is valuable because, in practical scenarios, the array needs to reliably tell the difference between short-term increases in R.H. and the application of a water-based solution containing pesticides.

The sensing array can successfully separate between Nimrod, and R.H. for all tested flow rates, especially to the flow rate that led the R.H. to reach 90%. In addition, regarding the 25 °C a better discrimination in horizontal PCA axes is presented.



**Graphs.5&6.** PCA for experimental data sets Nimrod vs Humidity for 25 °C and 35°C



## 4. Conclusions

### Proposed Applications

- 01 Detection of pesticide levels in greenhouse environments.
- 02 Contribution to the quality control of harmful substance residues in fruits and vegetables.
- 03 Bio-sensor for the detection of **major biomarkers** associated with diseases in human breath.

Volatile organic compounds in human breath come in various types and are numerous in number. Sometimes, When a person is suffering from a disease, either a substance characteristic of that disease (biomarker) appears, or one of the components found in the breath of a healthy individual significantly increases in concentration. After reviewing the relevant research in this field, five substances are identified as biomarkers for many diseases: acetone, isopropanol, ethanol, decanal, and pentane.

Chemical sensors could potentially evolve into biosensor devices, provided that the detected substances in both applications are of a similar nature. However, significant limitations regarding the concentration and liquid phase of these biomarkers must be considered.

| Biomarker         | Diseases        | Healthy Population Concentration | Patient Population Concentration | Unit of measurement |
|-------------------|-----------------|----------------------------------|----------------------------------|---------------------|
| Acetone           | Diabetes        | 0,4                              | 12                               | ppm                 |
| Acetone           | Type 1 Diabetes | 0,3 – 1                          | 1,5 – 2,5                        | ppm                 |
| Ethanol           | Lung Cancer     | 0,286                            | 0,467                            | ppm                 |
| Isopropyl alcohol | Lung Cancer     | 0,00197                          | 0,00741                          | ppm                 |

## 5. References

---

1. Kaloumenou, M. et al., 2022. Breath Analysis: A Promising Tool for Disease Diagnosis-The Role of Sensors. *Sensors*, 22(3), p. 1238.
2. Madianos, L. et al., 2018. Nanoparticle based gas-sensing array for pesticide detection. *Journal of Environmental Chemical Engineering*, 6(5), pp. 6641-6646.
3. Skotadis, E. et al., 2021. Identification of Two Commercial Pesticides by a Nanoparticle Gas-Sensing Array. *Sensors*, 21(17).
4. Skotadis, E., Tang, J., Tsouti, V. & Tsoukalas, D., 2010. Chemiresistive sensor fabricated by the sequential ink-jet printing deposition of a gold nanoparticle and polymer layer. *Microelectronic Engineering*, 87(11), pp. 2258-2263.
5. Skotadis, E. et al., 2015. Chemical sensing based on double layer PHEMA polymer and platinum nanoparticle films. *Sensors and Actuators B Chemical*, Issue 175, pp. 85-91.
6. Skotadis, E. et al., 2020. A sensing approach for automated and real-time pesticide detection in the scope of smart-farming. *Computers and electronics in Agriculture*, 178,
7. Amann , A. et al., 2014. The human volatilome: volatile organic compounds (VOCs) in exhaled breath, skin emanations, urine, feces and saliva. *Journal of Breath Research*, 8(3).